ELSEVIER

Contents lists available at ScienceDirect

International Journal of Pharmaceutics

journal homepage: www.elsevier.com/locate/ijpharm





Improved biocompatibility of dendrimer-based gene delivery by histidine-modified nuclear localization signals

Jeil Lee^a, Yong-Eun Kwon^b, Seth D. Edwards^a, Hwanuk Guim^c, Kyung Jae Jeong^{a,*}

- ^a Department of Chemical Engineering, University of New Hampshire, Durham, New Hampshire 03824, United States
- b Center for Scientific Instrumentation, Korea Basic Science Institute, 169-148 Gwahak-ro, Yuseong-gu, Daejeon 34133, Republic of Korea
- c Research Center for Materials Analysis, Korea Basic Science Institute, 169-148 Gwahak-ro, Yuseong-gu, Daejeon 34133, Republic of Korea

ARTICLE INFO

Keywords:
Nonviral vector
Cationic polymer
polyamidoamine (PAMAM) dendrimer
Transfection
Nuclear localization signal (NLS)

ABSTRACT

Polyamidoamine (PAMAM) dendrimers have been explored as an alternative to polyethylenimine (PEI) as a gene delivery carrier because of their relatively low cytotoxicity and excellent biocompatibility. The transfection efficiency of PAMAM dendrimers can be improved by the addition of nuclear localization signal (NLS), a positively charged peptide sequence recognized by cargo proteins in the cytoplasm for nuclear transport. However, increased positive charges from NLS can cause damage to the cytoplasmic and mitochondrial membranes and lead to reactive oxygen species (ROS)-induced cytotoxicity. This negative effect of NLS can be negated without a significant reduction in transfection efficiency by adding histidine, an essential amino acid known as a natural antioxidant, to NLS. However, little is known about the exact mechanism by which histidine reduces cytotoxicity of NLS-modified dendrimers. In this study, we selected cystamine core PAMAM dendrimer generation 2 (cPG2) and conjugated it with NLS derived from Merkel cell polyomavirus large T antigen and histidine (n = 0-3) to improve transfection efficiency and reduce cytoxicity. NLS-modified cPG2 derivatives showed similar or higher transfection efficiency than PEI 25 kDa in NIH3T3 and human mesenchymal stem cells (hMSC). The cytotoxicity of NLS-modified cPG2 derivatives was substantially lower than PEI 25 kDa and was further reduced as the number of histidine in NLS increased. To understand the mechanism of cytoprotective effect of histidineconjugated NLS, we examined ROS scavenging, hydroxyl radical generation and mitochondrial membrane potential as a function of the number of histidine in NLS. As the number of hisidine increased, cPG2 scavenged ROS more effectively as evidenced by the hydroxyl radical antioxidant capacity (HORAC) assay. This was consistent with the reduced intracellular hydroxyl radical concentration measured by 2',7'-dichlorodihydrofluorescein diacetate (DCFDA) assay in NIH3T3. Finally, fluorescence imaging with JC-1 confirmed that the mitochondrial membranes of NIH 3T3 were well-protected during the transfection when NLS contained histidine. These experimental results confirm the hypothesis that histidine residues scavenge ROS that is generated during the transfection process, preventing the excessive damage to mitochondrial membranes, leading to reduced cytotoxicity.

1. Introduction

Gene therapy became a realistic therapeutic method since Glybera and Imlygic, approved by European Union and the United States in 2010s (Hoh, 2023; Ma et al., 2020). Currently, most of the genetic medicines approved by the Food and Drug Administration (FDA) are virus-based vectors (Ma et al., 2020). Despite excellent targeting capacity and gene delivery efficiency, high production costs, and health risks for excessive immunogenicity, inflammatory reaction, potential carcinogenesis, and mutagenesis of virus-based vectors demand other

alternatives (Wang et al., 2021).

Nonviral vectors are typically made of cationic polymers, cationic lipids, and inorganic nanoparticles and have advantages such as ease of surface modification and quality control, and low immunogenicity and production cost. However, nonviral vectors suffer from significantly lower gene delivery efficiency than the viral vectors due to the absence of a specific delivery mechanism into the nuclei (Lächelt & Wagner, 2015). Only about 40 % of the polyplexes (i.e. a complex between DNA and cationic polymers) are endocytosed, and about 3 % of those reach the nuclear region (Clamme et al., 2003; Cohen et al., 2009; Glover

E-mail address: KyungJae.Jeong@unh.edu (K. Jae Jeong).

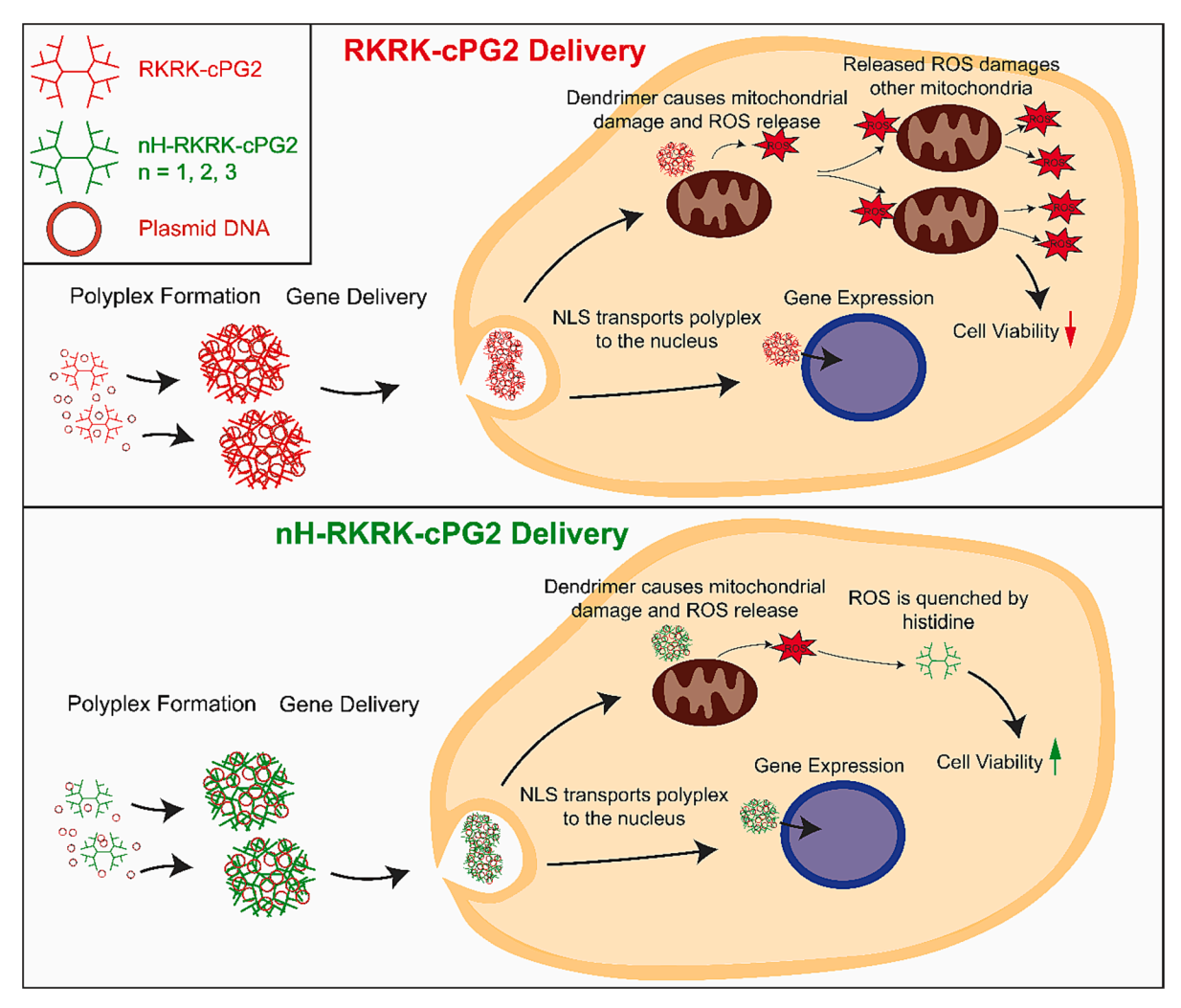
^{*} Corresponding author.

et al., 2010; Pollard et al., 1998; Shi et al., 2013b). Despite the recent advancement of mRNA-based gene therapies, which circumvent the necessity of the nuclear delivery of genetic materials, DNA-based gene delivery to the cell nucleus is still relevant for its more stable and long-term therapeutic effects (Ebenezer et al., 2023; Lewis et al., 2023; Mullard, 2023; Watts & Corey, 2012).

The nuclear distribution of polyplexes and therapeutic gene expression can be improved by the modification of cationic polymers with a nuclear localization signal (NLS), which is a peptide with a high content of positively charged amino acids. NLS facilitates the transport of polyplexes to the vicinity of the nucleus, increasing the chance of the gene to be transferred inside the nucleus during the nuclear envelope breakdown in mitosis (Hu et al., 2012; Park et al., 2015; Ren et al., 2012; Yi et al., 2012; Zhang et al., 2013).

One downside of NLS modification is increased cytotoxicity caused by the excessive amine groups on NLS which leads to the disruption of plasma membrane and other cellular organelles (e.g. mitochondria) (Jevprasesphant et al., 2003; Monnery et al., 2017). Polyethylenimine (PEI), poly-L-lysine, and high molecular weight chitosan share similar toxicity issues despite improved delivery efficiency (Fernandes et al., 2012; Kim et al., 2013; Symonds et al., 2005). Several strategies have been devised to overcome the cytotoxicity induced by increased positive charges, including ternary complexation of polyplex with anionic polymers and introduction of pH-sensitive linkages (e.g. ester, β -aminoester, schiff bases) which showed some improvement (Guo et al., 2017; Nam et al., 2009; Shi et al., 2013a; Zugates et al., 2006).

It has been found that addition of histidine residues to cationic polymers reduced induced cytotoxicity by increased positive charges (Bertrand et al., 2011; Mallick & Choi, 2015). Histidine acts as antioxidant by binding to metal ions and reducing the production of intracellular hydroxyl radicals and by directly scavenging singlet oxygen (Wade & Tucker, 1998). However little is known about the exact mechanism of histidine-mediated cytoprotection in the context of gene delivery and the quantitative effects of histidine on cytotoxicity and transfection efficiency. The main objective of this research is to measure the effect of number of histidine on cytotoxicity during the transfection by NLS-modified PAMAM dendrimers. We also aimed to elucidate on the mechanism of improved cytotoxicity by histidine-modified NLS. Our main hypothesis is that histidine protects the mitochondrial membranes from the reactive oxygen species (ROS) during the transfection (Scheme 1). The rationale for this hypothesis is the fact that histidine has the capacity to scavenge hydroxyl radicals (Hawkins & Davies, 2001; Vera-Aviles et al., 2018; Wade & Tucker, 1998). To prove this hypothesis and develop a highly effective non-viral gene delivery vehicle, we modified cystamine core PAMAM dendrimer of generation 2 (cPG2), with the NLS sequence derived from Merkel cell polyomavirus large T antigen, RKRK (Nakamura et al., 2010). We evaluated the antioxidant capacity of histidine-modified NLS (n = 0-3) and the mechanism of cytoprotective effects of histidine during the non-viral gene delivery.



Scheme 1. Schematic diagram illustrating mechanism of cytotoxicity and transfection efficiency of cPG2 derivatives conjugated with histidine-modified NLS.

2. Experimental

2.1. Materials

STARBURST® Poly(amidoamine) (PAMAM) dendrimer, Generation 2 - Cystamine Core - Amine Surface were bought from Andrews ChemServices (Berrien Springs, MI, USA). N,N-dimethylformamide dimethylsulfoxide (DMSO), N,N-diisopropylethylamine (DIPEA), Polyethylenimine (branched, 25 kDa), piperidine, triisopropylsilane (TIS), and trifluoroaceticacid (TFA), were purchased from Sigma-Aldrich (Burlington, MA, USA). N-Hydroxybenzotriazole (HOBt), 2-(1H-benzotriazole-1-yl)-1,1,3,3-tetra-methyluronium (HBTU), Fmoc-Arg(pbf)-OH, Fmoc-Lys(Boc)-OH, Fmoc-His(trt)-OH, were obtained from Anaspec (San Jose, CA, USA). Luciferase Assay System and Reporter Lysis 5X Buffer were bought from Promega (Madison, WI, USA). Alexa 546 Nucleic Acid Labeling Kit, AlamarBlue, DAPI (4',6-Diamidino-2-Phenylindole, Dihydrochloride), Dulbecco's modified eagle's medium (DMEM), Dulbecco's phosphate-buffered saline (DPBS), Fetal bovine serum (FBS), JC-1 Dve (Mitochondrial Membrane Potential Probe), Hanks' Balanced Salt Solution (HBSS), Micro BCA Protein Assay Kit, Quant-iTTM PicoGreenTM dsDNA Reagent, TrypLETM Express, Penicillin-Streptomycin were obtained from Thermo Fisher Scientific (Waltham, MA, USA). DCFDA/H2DCFDA - Cellular ROS Assay Kit was obtained from abcam (Waltham, MA, USA). HORAC Microplate Assay Kit was purchased from Eagle Biosciences (Amherst, NH, USA). NIH 3T3 and hMSCs were purchased from ATCC (Manassas, VA, USA). The luciferase expression plasmid DNA (pCN-Luci) was made as reported previously (Lee et al., 2002).

2.2. Synthesis of the cPG2 derivative conjugated with NLS and histidine

The synthesis of RKRK-cPG2 was performed as described in the previous study (Lee et al., 2021). Briefly, the cPG2 (10 mg), dried by nitrogen gas was lyophilized for 16 h. Conjugation of the NLS sequence was performed by mixing lyophilized cPG2, 4 eq. of Fmoc-Lys(Boc)-OH, HOBt, and HBTU, and 16 eq. of DIPEA in an anhydrous mixture of N,Ndimethylformamide (DMF)/dimethyl sulfoxide (DMSO) (2:1, v/v) as a total volume of 3 mL. The mixture solution was stirred at 37 °C for 18 h. Subsequently, Fmoc-Lys(Boc)-grafted cPG2 was precipitated and washed by cold diethyl ether and dried with nitrogen. The washing and reprecipitation steps were performed twice and centrifugation steps of 759 rcf for 3 min were performed for separation between precipitate and diethyl ether. The washed Fmoc-Lys(Boc)-grafted cPG2 was dissolved in piperidine solution (30:70, piperidine/DMF, v/v) as a total volume of 2.5 mL and stirred at 37 °C for 2 h for Fmoc deprotection. The deprotected cPG2 derivative was precipitated, washed, and dried in the same way. Conjugation steps of the next amino acids were performed as mentioned above. In cases of synthesis of RKRKH-cPG2, RKRKHH-cPG2, RKRKHHH-cPG2, lysine, and arginine were sequentially conjugated after conjugation of Fmoc-his(trt)-OH. Lastly, the deprotection of Boc, trt, and pbf protection groups was performed after the conjugation of all amino acids. The fmoc-depretected cPG2 derivatives were dissolved in a mixture solution (95:2.5:2.5, trifluoroacetic acid/triisopropylsilane/ distilled water, v/v/v) as a total volume of 4 mL and stirred for 8 h at 25 °C. The finally deprotected cPG2 derivatives were precipitated, washed, and dried in the same way. cPG2 derivatives were dissolved in distilled water in a total volume of 2 mL and dialyzed for 1 day. RKRKcPG2 and RKRKH-cPG2 were placed in tubing (Spectra/Por, molecular weight cut-off of 3,500) and RKRKHH-cPG2, RKRKHHH-cPG2 were transferred to tubing of molecular weight cut-off of 10,000. The dialyzed cPG2 derivatives were obtained as white powders after lyophilization. The conjugation yields of final products were dissolved in deuterium oxide (D₂O) and analyzed using 500 MHz ¹H nuclear magnetic resonance (NMR) spectroscopy (Bruker, Billerica, MA, USA).

2.3. PicoGreen exclusion assay for characterization of DNA complexation

cPG2 and cPG2 derivatives of various concentrations mixed with pCN-Luci (0.5 $\mu g)$ and incubated for 30 min to form polyplexes. All polyplexes were prepared at weight ratios ranging from 0.5:1 to 16:1. Formed polyplexes were diluted by 0.25 % PicoGreen solution (0.25:49.75:50, PicoGreen reagent/TE buffer/HEPES buffer, v/v/v) in a total volume of 400 μL . Each polyplex solution (20 $\mu L)$ and 80 μL of TE buffer (10 mM Tris, 1 mM EDTA, pH 7.5) were placed in 96-well plates, and fluorescence intensities of PicoGreen reagent were measured by excitation and emission wavelengths of 490 and 520 nm using by Synergy H1^M Hybrid Multi-Mode Microplate Reader (BioTek Instrument, Inc., Winooski, VT, USA).

2.4. Acid-base titration assay

The buffing capacity of cPG2 derivatives, PEI 25 kDa, and cPG2 was measured by acid-base titration. Each polymer (2 \times 10 $^{-7}$ mol) was prepared in the mixture solution (4 mL of 150 mM NaCl, 900 μ L of the respective polymers, and 1 N NaOH (100 μ L) and prepared in a total volume of 5 mL (120 mM NaCl solution). 20 μ L aliquots of 0.1 N hydrogen chloride (HCl) were titrated to each mixture solution. Experiments were performed until the pH reached 3 using Fisher Science Education TM Laboratory Benchtop pH Meters (Thermo Fisher Scientific, Waltham, MA, USA). Buffering capacity (β) of each polymer was calculated according to $\beta = dn(OH)/dpH$.

2.5. Diameter and ζ -potential analysis of polyplexes

To measure the diameter and ζ -potentials of polyplexes, each polyplex was prepared by mixing pCN-Luci (2 μ g) and polymer of various concentrations and incubated for 30 min. Each polymer /pCN-Luci polyplexes were prepared at weight ratios ranging from 0.5:1 to 12:1. Prepared polyplexes were diluted in a total volume of 1.6 mL (distilled water) and were measured at 25 °C using Zeta-potential & Particle Size Analyzer ZetaPALS (Brookhaven Instruments, Holtsville, NY, USA).

2.6. Scanning transmission electron microscopy (-in-SEM) imaging and low-voltage energy dispersive X-ray spectroscopy (EDS) analysis

The respective polymer/pCN-Luci polyplexes were prepared in a total volume of 10 μL at a weight ratio of 12:1 and incubated for 30 min. Prepared polyplexes were diluted by 75 % ethanol solution (75:25, ethanol/water, v/v) in a total volume of 800 μL . 2 μL of each polyplex was dropped at the 200-mesh ultra-thin carbon-supported copper grids and dried at 60 °C for 16 h. Field emission scanning electron microscope (FE-SEM) images polyplexes were observed under the conditions of dark-field image mode, 30 kV using Merlin Compact (Carl Zeiss Inc., Oberkochen, Germany). EDS analysis (XFlash 6160, Bruker; takeoff angle: 35°; detector area 60 mm³) spectra of polyplexes were obtained under the condition of 10 kV, 8.3 mm of working distance (WD), and 100 s of analysis time.

2.7. Cell culture

NIH3T3 mouse embryonic fibroblast cells were cultured in the DMEM growth medium (89:10:1, DMEM/FBS/Penicillin-Streptomycin, v/v/v). Human mesenchymal stem cells (hMSC) were cultured in the $\alpha\textsc{-MEM}$ growth medium (89:10:1, $\alpha\textsc{-MEM/FBS/}$ Penicillin-Streptomycin, v/v/v). Two types of cells were cultured in Nunc EasY-Flask 75 cm² (Thermo Fisher Scientific, Portsmouth, NH, USA) at 37 °C in a humidified atmosphere (5 % CO2/95 % air, v/v).

2.8. Transfection assay

NIH3T3 and hMSC cells were seeded in 96-well plates and 48-well

plates at a density of 1.8×10^4 cells/well and 1.0×10^4 cells/well respectively. When cells reached 70-80 % confluency in 16 h, cPG2 derivatives/pCN-Luci polyplexes were added to cells. Each polyplex was prepared by mixing pCN-Luci (0.5 µg) and polymers of various concentrations in a total volume of 30 µL and incubated for 30 min. polyplexes of cPG2 derivatives were formed as weight ratios ranging from 4:1 to 16:1 to confirm optimal transfection efficiency. Polyplexes of cPG2 and PEI 25 kDa were prepared as weight ratios 16:1 and 1:1 and these weight ratios indicate optimal transfection efficiency. Polymer concentrations of polyplexes prepared as 1:1, 4:1, 8:1, 12:1, and 16:1 wt ratios are 3.85, 15.4, 30.8, 46.2, and 61.5 $\mu g/mL$. Cells treated with polyplexes were incubated for 1 day. Transfected cells were washed with 100 μL of DPBS and 100 μL of the reporter lysis buffer (1 mg/mL) was added per well. 96-well plates and 48-well plates were incubated in a shaker at 150 rpm for 30 min at room temperature. The lysate was transferred to microtubes and centrifuged at 15,000 rcf for 10 min. The supernatant of lysed cells was placed in microtubes. Luciferase activities were measured by mixing 10 µL of each lysate and 10 µL luciferin using the Lumat LB 9507 instrument (Berthold Technology, Bad Wildbad, Germany), and protein concentrations of lysate containing luciferase were analyzed using a Micro BCATM protein assay kit. The absorbance of BCA solution at 570 nm using Synergy H1TM Hybrid Multi-Mode Microplate Reader (BioTek Instrument, Inc., Winooski, VT, USA). Finally, the transfection efficiency of cPG2 derivatives, cPG2, and PEI 25 kDa was calculated as a relative light unit (RLU) per microgram of total protein.

2.9. Cytotoxicity assay

Cytotoxicity resulting from polymer concentrations was measured using the alamarBlue assay. NIH3T3 and hMSC cells were seeded in 96-well plates at a density of 1.8×10^4 cells/well and 1.0×10^4 cells/well respectively and incubated for 16 h. cPG2 derivatives, cPG2, and PEI 25 kDa prepared as concentrations ranging from 10 to 160 µg/mL were added to cells reached by 70–80 % confluency and incubated for 1 day. Then, 10 µL of alamarBlue reagent was added per well and incubated for 2 h. Relative fluorescence intensities of the alamarBlue reagent were measured by excitation and emission wavelengths of 560 and 590 nm using Synergy H1 $^{\rm TM}$ Hybrid Multi-Mode Microplate Reader (BioTek Instrument, Inc., Winooski, VT, USA).

2.10. Confocal microscopy of polyplexes using Alexa Fluor 546-labeled pCN-Luci

The pCN-Luci was labeled by Alexa Fluor 546 as described in the manufacturer's protocol. NIH3T3 cells were seeded at a density of 2.0 imes10⁴ cells/well in a 1μ-Slide 8 well (Ibidi) and incubated for 1 day. Polyplexes of cPG2 derivatives, cPG2, and PEI 25 kDa were prepared as described in the transfection assay section, treated to cells, and incubated for 1 day. cPG2, RKRKHH-cPG2/pCN-Luci polyplexes were at a weight ratio of 16:1, RKRK-cPG2, RKRKH-cPG2, and RKRKHHH-cPG2/ pCN-Luci polyplexes were at a weight ratio of 12:1 and PEI 25 kDa/pCN-Luci polyplexes were at a weight ratio of 1:1. These ratios indicated optimal efficiency in transfection assay. Before 2 h for observation of confocal microscope, DAPI was treated in cells at a total concentration of 20 μg/mL for nucleus staining. Subsequently, the growth media were removed, and cells were washed by DPBS twice. Finally, 200 µL of HBSS was added per well and cellular images were obtained using a Nikon A1R Laser Scanning Confocal Fluorescence Microscope. The relative fluorescence intensity (F.I) of polyplex distributed near the nucleus was calculated as

$$\textit{RedF.Iinperinuclearregion} = \frac{\textit{locatedDNAF.Iwithin2.5} \mu \textit{mnearnuclei}}{\textit{Thenumberofnuclei}}$$

2.11. Hydroxyl radical antioxidant capacity (HORAC) assay

The Hydroxyl radical scavenging capacity of cPG2 derivatives was analyzed using HORAC assay and performed as described in the manufacturer's protocol. Briefly, cPG2 and cPG2 derivatives were prepared at concentrations ranging from 25 to 200 $\mu M.$ 20 μL aliquots of each polymer were added to 96-well plates and 140 μL of the fluorescein working solution, 20 μL of the hydroxyl radical, and 20 μL of the Fenton reagent were added in sequence. Fluorescent intensities of the mixture were analyzed by excitation and emission wavelengths of 560 and 590 nm and change of the intensity was measured every 5 min. The relative fluorescence intensity was calculated as

$$\textit{Relative fluorescence intensity}(\%) = \frac{\textit{Final F.I.}}{\textit{Initial F.I.}} \times 100$$

2.12. Dichlorodihydrofluorescein diacetate (DCFDA) assay

The mitigation capacity of cPG2 derivatives by intracellular hydroxyl radical was evaluated by DCFDA assay. NIH3T3 cells were seeded in 96-well plates at a density of 2.5×10^4 cells/well and incubated for 1 day. Each polymer was diluted at a concentration of 50 μM in the DMEM growth medium of 20 μM DCFDA. The growth medium of cells was replaced by fresh growth media containing polymer and DCFDA and incubated for 2 h. Cells were washed with 100 μL of HBSS twice. Finally, 100 μL of HBSS was treated again and fluorescence intensities were detected by excitation and emission wavelengths of 485 and 535 nm. Fluorescence microscope images of the cells were observed using EVOS FL Imaging System (Thermofisher, Waltham, MA) after microplate analysis. The normalized fluorescence intensity was calculated as

$$normalized fluorescence intensity (F.I) = \frac{sample F.I - negative control F.I}{Postive control F.I}$$

Cells treated with 55 μ M of *tert*-Butyl hydroperoxide (TBHP) and 20 μ M of DCFDA were used as positive control and negative control was only fluorescence intensity of 20 μ M of DCFDA.

2.13. JC-1 assay

The mitochondrial condition resulting from cPG2 derivatives was evaluated by JC-1 assay. NIH3T3 cells of a density of 1.8×10^4 cells/well were seeded in 96-well plates and incubated for 16 h. The respective polymers were prepared at a concentration of 50 μM in the DMEM growth medium. The cellular growth medium of cells, reached by 70–80 % confluency was replaced by 100 μL of fresh growth media diluted by each polymer and incubated for 1 day. Subsequently, the cellular growth medium was replaced with fresh growth medium diluted by 3 μM JC-1 reagent and incubated for 30 min. Cells were washed with 100 μL of HBSS twice and replenished. Fluorescence microscope images were obtained using EVOS FL Imaging System (Thermofisher, Waltham, MA).

2.14. Statistical analysis

Statistical analysis of the experimental data was performed using GraphPad Prism 5 software. Significant differences among the groups were evaluated by one-way analysis of variance (ANOVA) with Dunnett's Multiple Comparison Test for the transfection efficiency test or Tukey post hoc test for HORAC, DCFDA and JC-1 analyses: *p < 0.05, **p < 0.01, and ***p < 0.001.

3. Result and discussion

3.1. Synthesis and characterization of cPG2 derivatives

The modification of NLS and histidine to cPG2 was performed by conjugating and deprotecting amino acids sequentially using HOBt and $\frac{1}{2}$

HBTU coupling reaction as described in the experimental section and Scheme S1. The relative conjugation yield of NLS and histidine and the total molecular weight of cPAMAM derivatives were calculated using ¹H NMR spectroscopy (Table 1, Table S1 and Fig. S1). The final conjugation yields of all cPG2 derivates were comparable (84 %, 88 %, 85 % and 84 % for RKRK-cPG2, RKRKH-cPG2, RKRKHH-cPG2 respectively).

Next, we evaluated the proton buffering capacity of cPG2 derivatives (Fig. S2). The protonating property of amine groups present in cationic polymers leads to endosome disruption by inducing osmotic imbalance during endosome maturation which is an important factor to increase the nuclear entry of plasmid DNA. We compared cPG2 derivatives with PEI (MW 25 kDa) since PEI has been the most widely used non-viral vector. PEI, having the highest number of amines per molecule, showed the best proton buffering capacity. Proton buffering capacity of cPG2 derivatives was dependent on the amount of histidine due to the protonation capacity of the imidazole group at physiological pH.

3.2. Physical characteristics of cPG2 derivatives/pCN-Luci polyplexes

Cationic polymers aid in gene delivery by condensing plasmid DNA into nanoscale particles, called polyplexes, and reducing electrostatic repulsion with the cellular membrane by neutralizing the negative charges of plasmid DNA. To confirm the weight ratios of cPG2 derivatives to plasmid DNA for stable polyplex formation, we analyzed the polyplexes by PicoGreen exclusion assay.

Polyplex formation results in significant decrease in fluorescence of the PicoGreen reagent as it is excluded from the plasmid DNA (Choi et al., 2004; Geall & Blagbrough, 2000). cPG2 derivatives and the plasmid DNA (pCN-Luci) were beginning to form stable polyplexes at a weight ratio of 4:1 (polymer:DNA) evidenced by the near zero fluorescence (Fig. 1A). This trend was unaffected by the amount of histidine, likely because the imidazole groups are in a deprotonated form and had little impact on electrostatic interactions with plasmid DNA.

Polyplexes were further characterized by scanning transmission electron microscopy (-in-SEM) and energy-dispersive X-ray spectroscopy (EDS). Under the STEM images, polyplexes were spherical in shape and had a size distribution ranging from 100 to 250 nm (Fig. 1B). EDS analysis confirmed that the nanoparticles in the STEM images were polyplexes with the peaks from phosphorous, an intrinsic element of DNA, and carbon, nitrogen, and oxygen from cPG2 derivatives (Fig. S3). Occasionally polymer aggregates without DNA were also observed.

The size and ζ -potential of polyplexes are considered important physical properties associated with binding affinity with the plasma membrane and cellular uptake by endocytosis thereby influencing the transfection efficiency. The average size of polyplexes was suitable for endocytosis (<300 nm) with relatively low polydispersities (<0.5), and a gradual size decrease was observed as the polymer to DNA weight ratio increased from 0.5:1 to 16:1 (Fig. 1C and Table S2). ζ -potentials of the polyplexes made of cPG2 derivatives (i.e. cPG2 conjugated with NLS) were lower than those of polyplexes made of unmodified cPG2 (Fig. 1D). This trend can be explained by the fact that cPG2 derivatives, having a

Table 1 Relative molecular weight calculated by $^1\mathrm{H}$ NMR, and charge numbers.

Sample	MW (Da)	No. of +charge/polymer	No. of +charge/ μ g ^c
cPG2	3348.4 ^a	16	2.9×10^{15}
RKRK-cPG2	11823 ^b	76	3.9×10^{15}
RKRKH-cPG2	13678 ^b	74	2.3×10^{15}
RKRKHH-cPG2	15625 ^b	74	2.9×10^{15}
RKRKHHH-cPG2	17298 ^b	74	2.6×10^{15}

- ^a Molecular weight is provided by the manufacturer.
- ^b Molecular weight is calculated by ¹H NMR.

higher number of positive charges than unmodified cPG2, requiring fewer polymers to form stable polyplexes with the plasmid DNA, leading to the lower ζ -potentials.

3.3. In vitro cytotoxicity evaluation of cPG2 derivatives

The cytotoxicity of gene carriers should be minimized in the transfected cells for the stable and continuous expression of therapeutic proteins. AlamarBlue assay was performed to evaluate in vitro cytotoxicity for NIH 3T3 and human mesenchymal stem cells (hMSCs) as a function of polymer (PEI, cPG2 or cPG2 derivatives) concentration (Fig. 2). In general, cPG2 derivatives showed lower cytotoxicity than PEI. However, for the low histidine cPG2 derivates (RKRK-cPG2 and RKRKH-cPG2), there was substantial increase in cytotoxicity at polyplex concentrations higher than 40 µg/mL and 10 µg/mL in NIH 3T3 and hMSC, respectively. The high histidine cPG2 derivatives (RKRKHHcPG2 and RKRKHHH-cPG2) exhibited much lower cytotoxicity for both cell types. These results clearly show that the addition of histidine to NLS significantly improves biocompatibility of dendrimer-based gene carriers likely due to its antioxidant property. This is consistent with other related studies in which histidine-modified cationic polymers showed reduced cytotoxicity(Benns et al., 2000; Bertrand et al., 2011; Chang et al., 2011; Mallick & Choi, 2015) and histidine-containing peptides exhibiting antioxidant effects (Wake et al., 2020).

3.4. Transfection efficiency and intracellular distribution of cPG2 derivatives/pCN-Luci polyplexes

Transfection efficiency of cPG2 derivatives were evaluated at various polymer to DNA weight ratios (4:1 – 16:1) using the NIH3T3 and hMSCs (Fig. 3A). The results were compared to the transfection by PEI at 1:1 polymer to DNA ratio, which is known to be an optimal composition for transfection for PEI (Zhang et al., 2018). Transfection efficiency for each cPG2 derivative was a function of polymer to DNA weight ratio, and only the case of maximum transfection is shown in Fig. 3A. The entire data set can be found in Fig. S4. cPG2 derivatives achieved roughly two orders of magnitude higher transfection efficiency than unmodified cPG2, and similar or higher transfection efficiency than PEI in both cell types. For NIH 3 T3, the high histidine cPG2 derivatives (RKRKHH-cPG2 and RKRKHHH-cPG2) resulted in slightly lower transfection efficiencies than the low histidine cPG2 derivatives (RKRK-cPG2 and RKRKH-cPG2) However, their transfection efficiencies were still higher than or comparable to that of PEI. For hMSCs, the high histidine groups showed slightly higher transfection efficiencies than the low histidine groups and were significantly higher than PEI (p < 0.001).

NLS modification of cPG2 is known to facilitate transfection efficiency by targeting cargo proteins (e.g. importin, karyopherin) after the endosomal escape and promoting the localization of polyplexes at the nucleus (Kirby et al., 2017; Wing et al., 2022). The effect of NLS was visualized by the distribution of polyplexes in NIH 3 T3 cells using confocal microscopy (Fig. 3B). The polyplexes made of NLS-modified cPG2 resulted in much higher localization near the nuclei than the ones made of unmodified cPG2. A quantitative analysis of the fluorescence images clearly shows that NLS enhanced perinuclear localization of polyplexes and the addition of histidine did not affect this effect of NLS (Fig. S5). These results are consistent with the transfection efficiency of each polymer.

3.5. Influence evaluation of cPG2 derivatives on ROS

As was demonstrated above, conjugation of NLS (i.e. RKRK) to cPG2 improved the transfection efficiency (Fig. 3) but at the cost of increased cytotoxicity (Fig. 2), and addition of histidine residues to NLS substantially reduced cytotoxicity. We sought to understand the mechanism by which histidine provides protection to the cells. Our hypothesis was that histidine scavenges ROS that is produced during the transfection by the

^c The N/P ratio of each polyplex at 1:1 wt ratio (polymer:DNA) is 1.6 for cPG2, 2.1 for RKRK-cPG2, 1.8 for RKRKH-cPG2, 1.6 for RKRKHH-cPG2 and 1.4 for RKRKHHH-cPG2.

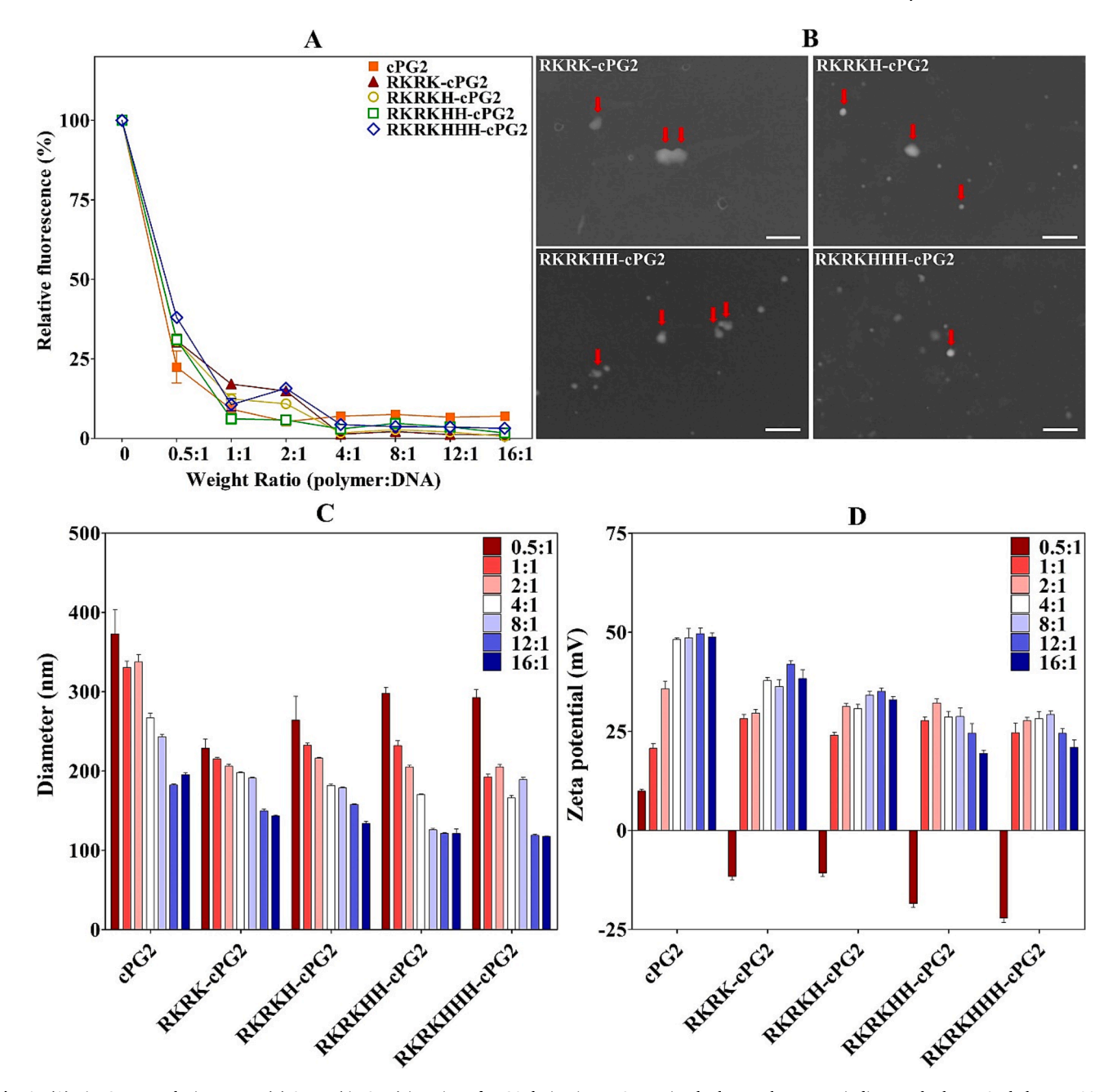


Fig. 1. (A) PicoGreen exclusion assay. (B) STEM (-in-SEM) imaging of cPG2 derivatives/pCN-Luci polyplexes. The arrows indicate polyplexes. Scale bar = 500 nm. (c)Size and (d) ζ -potential of polyplexes at various weight ratios. Data are shown as mean \pm standard deviation (n = 3).

positively charged cPG2 derivatives and protects the mitochondria.

Hydrogen peroxide (H_2O_2) is constantly generated in the electron transfer system of mitochondria during the ATP synthesis. Most of H_2O_2 is cleared by enzymes, such as superoxide dismutases (SODs) and catalase. However, the positively charged polymers can bind to and disrupt some of the mitochondrial membranes, leading to a rapid increase in H_2O_2 beyond the capacity of the neutralizing enzymes (El-Beltagi & Mohamed, 2013; Grandinetti et al., 2011; Lee et al., 2013; Macdonald et al., 2003; Xia et al., 2008). H_2O_2 in the cytoplasm can be converted to highly cytotoxic hydroxy radical (·OH) through Fenton reaction (Li et al., 2019) and facilitate cell death (Hunter & Moghimi, 2010; Li et al., 2019; Naha et al., 2010).

We first evaluated the antioxidant capacity of histidine-modified cPG2 derivatives in a physiological buffer using HORAC assay, which measures the protective effect of antioxidant molecules by the prevention of fluorescence quenching by the hydroxyl radical (Fig. 4 and Fig

S5). Modification with NLS alone (i.e. RKRK-cPG2) did not confer any antioxidant capacity to cPG2. The antioxidant capacity of histidine-modified cPG2 derivatives increased with the number of histidine residues (n = 1–3), and with the polymer concentrations (25–200 μM), evidenced by higher fluorescence signals over time. For the case of 200 μM polymer concentration, the difference of fluorescence intensity between RKRKHHH-cPG2 and RKRK-cPG2 was 41 % (78 \pm 3 % vs 37 \pm 3 %, p < 0.001).

Since histidine residues on NLS were demonstrated to have antioxidant capacity, we hypothesized that cPG2 conjugated with histidine-modified NLS would result in less intracellular hydroxyl radicals than cPG2 conjugated with NLS only. DCFDA assay enables visualization of the intracellular ROS by enhanced fluorescence of DCFDA in the presence of hydroxyl radicals (Fig. 5). Consistent with its well-known cytotoxic effect, PEI led to excessive intracellular ROS in NIH 3 T3. ROS generation was substantially reduced with RKRK-cPG2 compared to PEI,

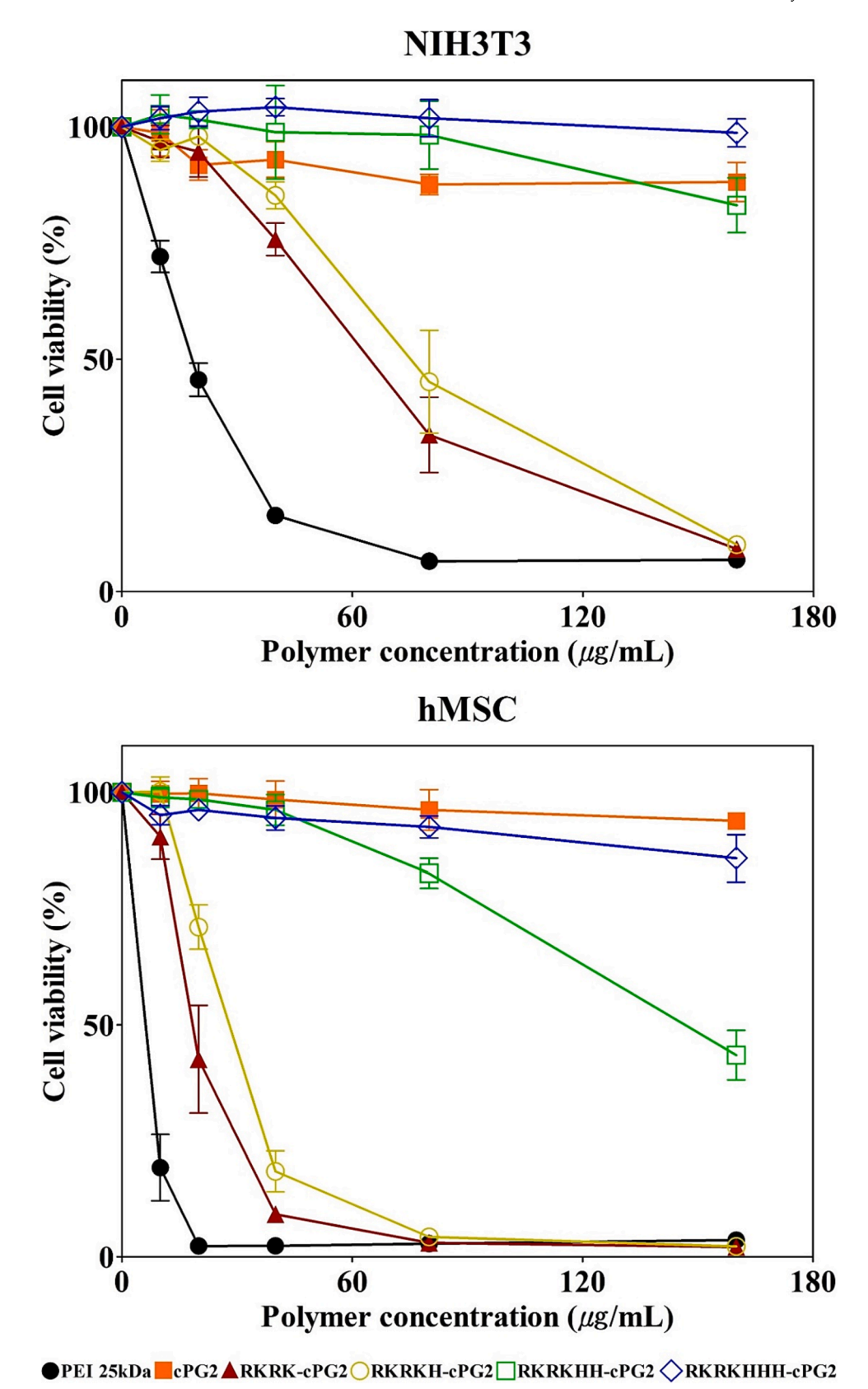


Fig. 2. Cytotoxicity assay in NIH 3 T3 and hMSC using alarmarBlue assay. Data are shown as mean \pm standard deviation (n = 3).

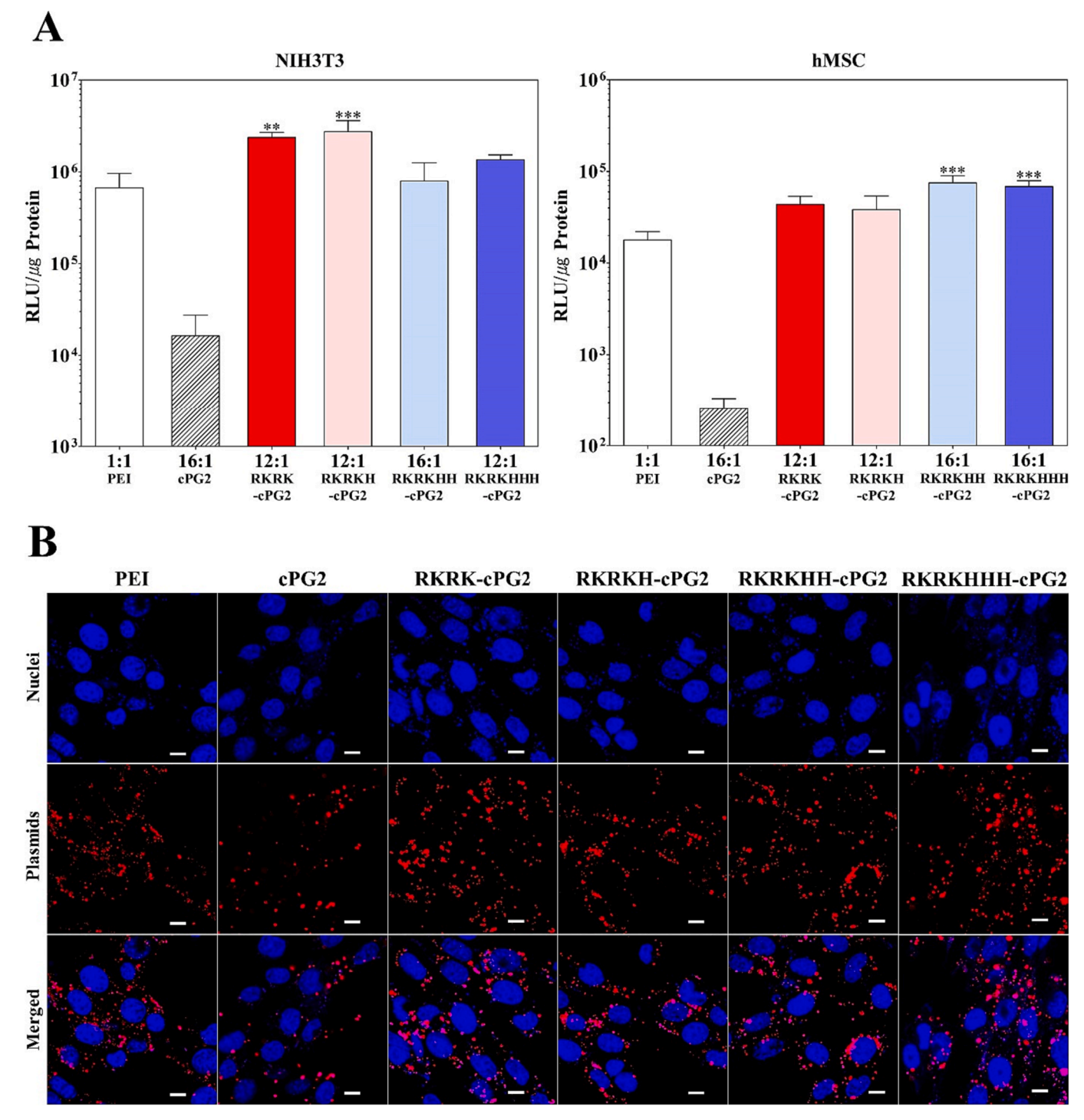


Fig. 3. (A) Transfection efficiency of cPG2 derivatives. Each weight ratio indicates the optimal transfection efficiency. (B) Confocal microscope images (NIH3T3 cells). Polymer concentrations of polyplexes prepared as 1:1, 12:1, and 16:1 wt ratios are 3.85, 46.2, and 61.5 μ g/mL. Cell nuclei and plasmid DNA were stained with DAPI (blue) and Alexa 546 (red), respectively. The images were taken using the optimal polymer to DNA ratios found in (a). Scale bar = 10 μ m.

which confirms superior biocompatibility of PAMAM dendrimer-based gene delivery vectors (Fig. S6). Addition of one histidine to NLS (RKRKH-cPG2) slightly increased intracellular ROS compared to RKRK-cPG2, which means there was not enough antioxidant capacity. When more histidine was added to NLS (RKRKHH-cPG2 and RKRKHHH-cPG2), no measurable ROS was detected by DCFDA assay. These results clearly demonstrate the antioxidant effect of histidine-modified NLS, suppressing the generation of cytotoxic intracellular ROS by the positively charged gene carriers.

Finally, we sought to demonstrate that the reduction of ROS by

histidine prevents mitochondrial injury caused by hydroxyl radicals using the JC-1 assay. JC-1 reagent is a fluorescence indicator of mitochondrial membrane potential: red and green fluorescence indicates high and low mitochondrial membrane potential, respectively. Cells treated with PEI showed damaged cellular morphologies (bright field) with a high green fluorescence intensity, meaning significant mitochondrial damage and cell death (Fig. S7). cPG2-based carriers showed much lower green fluorescence than PEI. As the number of histidine increased, green fluorescence intensity decreased, indicating minimal mitochondrial disruption, proving the protective effect of histidine

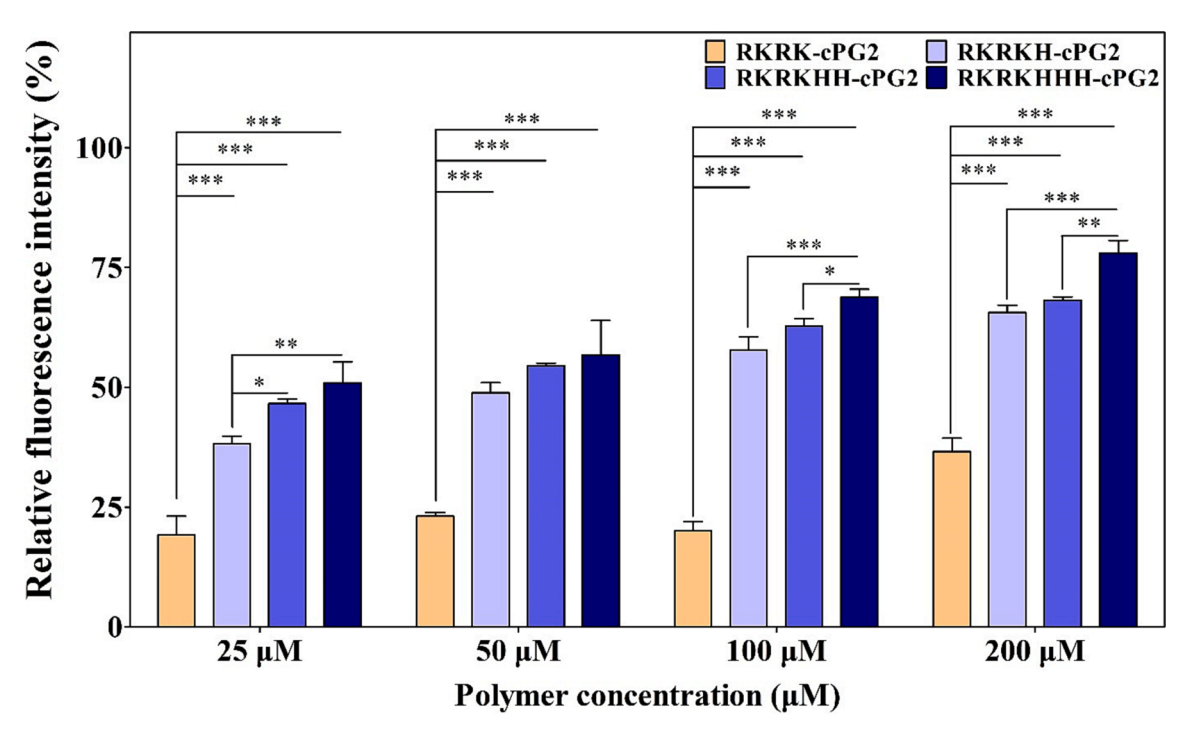


Fig. 4. Evaluation of hydroxyl radical scavenging capacity of cPG2 derivatives using HORAC assay. The control means a fluorophore without hydroxyl radical. Relative fluorescence intensity was evaluated after 1 h. *, ** and *** denote p < 0.05, p < 0.01 and p < 0.001, respectively.

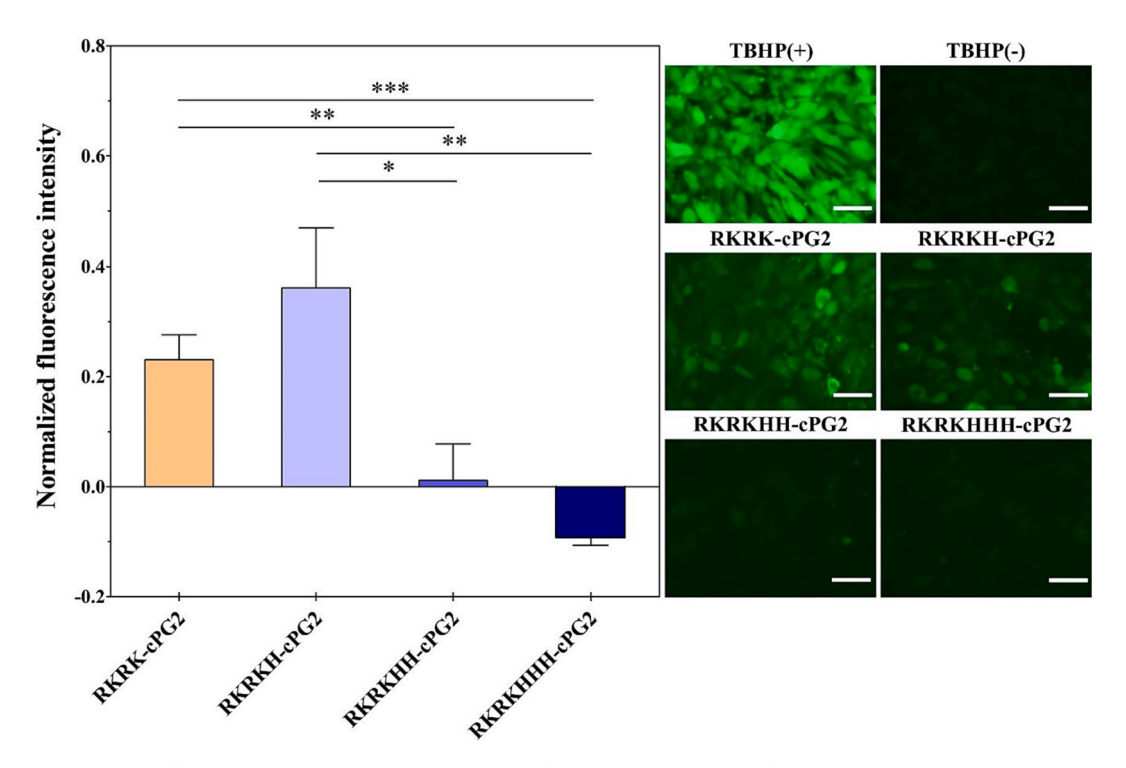


Fig. 5. DCFDA assay in NIH3T3 cells treated with cPG2 derivatives (50 μ M). Fluorescence images were obtained after the microplate reader measurements. (Scale bar = 50 μ m) Tert-butyl hydroperoxide (TBHP) is a positive control. *, ** and *** denote p < 0.05, p < 0.01 and p < 0.001, respectively.

against ROS (Fig. 6A). The quantitative analysis of green/red fluorescence confirms that the mitochondrial damage is reduced as the number of histidine increased (Fig. 6B), consistent with the observations from HORAC (Fig. 4) and DCFDA (Fig. 5) assays.

Taken together, the results in Figs. 4-6 confirm our original hypothesis that histidine residues scavenge hydroxyl radicals caused by the positively charged polymers, protect the mitochondria and minimize

cytotoxicity during the transfection.

4. Conclusion

In this study, we modified cPG2 with RKRK sequence, a NLS derived from Merkel cell polyomavirus large T antigen and histidine (n = 1–3) and evaluated the effect of the number of histidine residues on

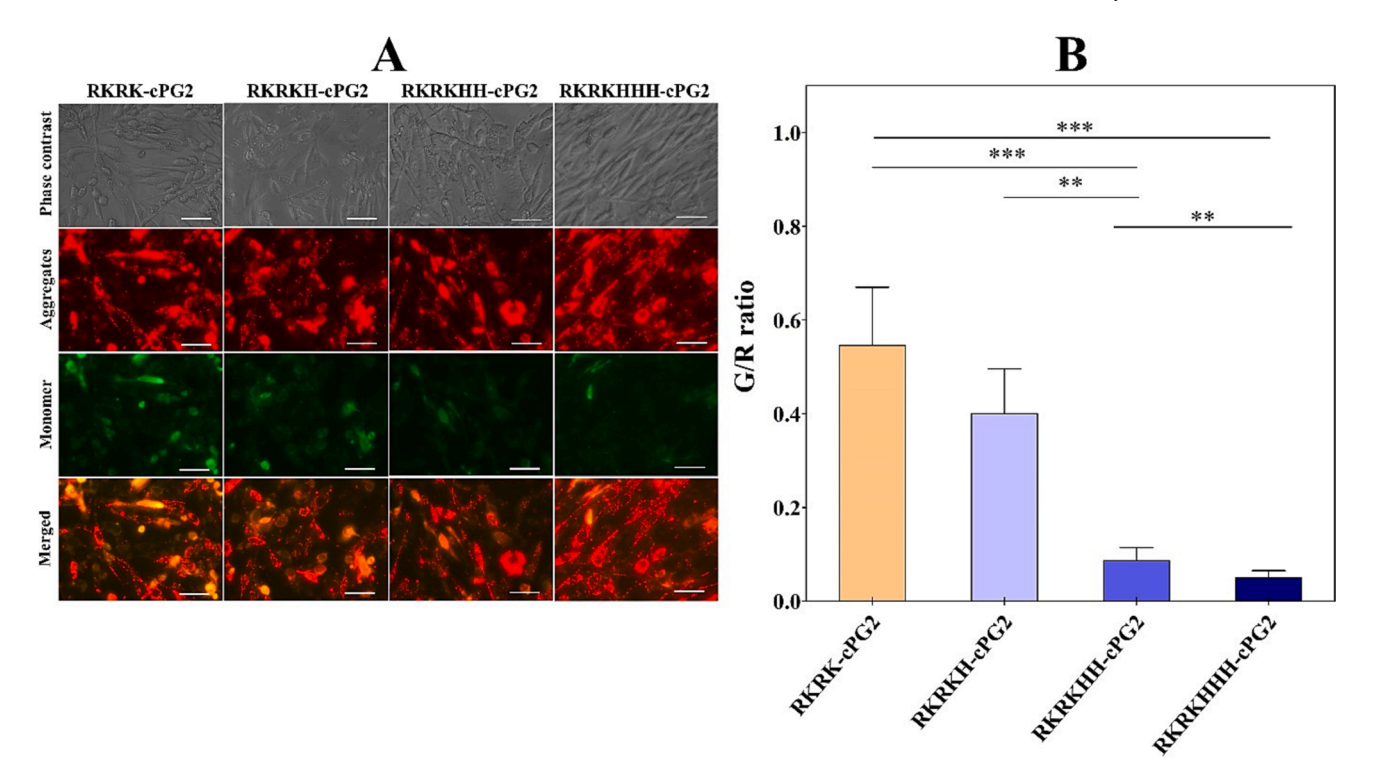


Fig. 6. (A) JC-1 assay images of NIH3T3 cells treated with cPG2 derivatives of 50 μ M. (Scale bar = 50 μ m) (B) Ratio of green to red fluorescence (G/R ratio). *, ** and *** denote p < 0.05, p < 0.01 and p < 0.001, respectively.

transfection efficiency and cytotoxicity of cPG2 derivatives. NLS-modified cPG2 derivatives showed comparable transfection efficiency to PEI for both a mouse cell line (NIH 3T3) and primary human stem cells (hMSCs), and the addition of histidine to NLS substantially reduced its cytotoxicity without affecting the transfection efficiency. Based on HORAC, DCFDA, and JC-1 assay, it was demonstrated that histidine-modified NLS had antioxidant capacity minimizing the generation of intracellular hydroxyl radical and preventing the mitochondrial damages, and the antioxidant effect was dependent on the number of histidine residues. Our results provide important design principles for the development of safe and effective non-viral gene carriers for gene therapy.

CRediT authorship contribution statement

Jeil Lee: Conceptualization, Validation, Formal analysis, Investigation, Writing – original draft, Visualization. Yong-Eun Kwon: Methodology, Investigation, Visualization. Seth D. Edwards: Methodology, Visualization. Hwanuk Guim: Methodology. Kyung Jae Jeong: Conceptualization, Methodology, Writing – review & editing, Supervision, Funding acquisition.

Declaration of Competing Interest

The authors declare the following financial interests/personal relationships which may be considered as potential competing interests: [Kyung Jae Jeong reports financial support, administrative support, and equipment, drugs, or supplies were provided by University of New Hampshire.].

Data availability

Data will be made available on request.

Acknowledgment

This research was sponsored by the U.S. National Science Foundation and was accomplished under the Grant No. OIA-1757371 and by the University of New Hampshire's Center for Integrated Biomedical and Bioengineering Research (CIBBR) through a grant from the National Institute of General Medical Sciences of the National Institutes of Health under Award Number P20GM113131.

Appendix A. Supplementary material

Supplementary data to this article can be found online at $\frac{https:}{doi.}$ org/10.1016/j.ijpharm.2023.123299.

References

Benns, J.M., Choi, J.-S., Mahato, R.I., Park, J.-S., Kim, S.W., 2000. pH-sensitive cationic polymer gene delivery vehicle: N-Ac-poly (L-histidine)-graft-poly (L-lysine) comb shaped polymer. Bioconjug. Chem. 11, 637–645.

Bertrand, E., Gonçalves, C., Billiet, L., Gomez, J.P., Pichon, C., Cheradame, H., Midoux, P., Guégan, P., 2011. Histidinylated linear PEI: a new efficient non-toxic polymer for gene transfer. Chem. Commun. 47, 12547–12549.

Chang, K.-L., Higuchi, Y., Kawakami, S., Yamashita, F., Hashida, M., 2011. Development of lysine–histidine dendron modified chitosan for improving transfection efficiency in HEK293 cells. J. Control. Release 156 (2), 195–202.

Choi, J.S., Nam, K., Park, J.-Y., Kim, J.-B., Lee, J.-K., Park, J.-S., 2004. Enhanced transfection efficiency of PAMAM dendrimer by surface modification with Larginine. J. Control. Release 99 (3), 445–456.

Clamme, J.P., Azoulay, J., Mély, Y., 2003. Monitoring of the formation and dissociation of polyethylenimine/DNA complexes by two photon fluorescence correlation spectroscopy. Biophys. J. 84 (3), 1960–1968.

Cohen, R.N., van der Aa, M.A.E.M., Macaraeg, N., Lee, A.P., Szoka, F.C., 2009. Quantification of plasmid DNA copies in the nucleus after lipoplex and polyplex transfection. J. Control. Release 135 (2), 166–174.

Ebenezer, O., Comoglio, P., Wong, G.-S., Tuszynski, J.A., 2023. Development of novel siRNA therapeutics: A review with a focus on Inclisiran for the treatment of hypercholesterolemia. Int. J. Mol. Sci. 24 (4), 4019.

El-Beltagi, H.S., Mohamed, H.I., 2013. Reactive oxygen species, lipid peroxidation and antioxidative defense mechanism. Notulae Botanicae Horti Agrobotanici Cluj-Napoca 41, 44–57.

- Fernandes, J.C., Qiu, X., Winnik, F.M., Benderdour, M., Zhang, X., Dai, K., Shi, Q., 2012. Low molecular weight chitosan conjugated with folate for siRNA delivery in vitro: optimization studies. Int. J. Nanomed. 5833–5845.
- Geall, A.J., Blagbrough, I.S., 2000. Rapid and sensitive ethidium bromide fluorescence quenching assay of polyamine conjugate–DNA interactions for the analysis of lipoplex formation in gene therapy. J. Pharm. Biomed. Anal. 22 (5), 849–859.
- Glover, D.J., Leyton, D.L., Moseley, G.W., Jans, D.A., 2010. The efficiency of nuclear plasmid DNA delivery is a critical determinant of transgene expression at the single cell level. J. Gene Med. 12 (1), 77–85.
- Grandinetti, G., Ingle, N.P., Reineke, T.M., 2011. Interaction of poly (ethylenimine)–DNA polyplexes with mitochondria: implications for a mechanism of cytotoxicity. Mol. Pharm. 8 (5), 1709–1719.
- Guo, A., Wang, Y., Xu, S., Zhang, X., Li, M., Liu, Q., Shen, Y., Cui, D., Guo, S., 2017. Preparation and evaluation of pH-responsive charge-convertible ternary complex FA-PEI-CCA/PEI/DNA with low cytotoxicity and efficient gene delivery. Colloids Surf. B Biointerfaces 152, 58–67.
- Hawkins, C.L., Davies, M.J., 2001. Generation and propagation of radical reactions on proteins. Biochim. Biophys. Acta (BBA)-Bioenerg. 1504 (2-3), 196–219.
- Hoh, Y.K., 2023. The First Three Decades of Gene Therapy: An Instant Update. Am. Biol. Teach. 85, 17–22.
- Hu, Q., Wang, J., Shen, J., Liu, M., Jin, X., Tang, G., Chu, P.K., 2012. Intracellular pathways and nuclear localization signal peptide-mediated gene transfection by cationic polymeric nanovectors. Biomaterials 33 (4), 1135–1145.
- Hunter, A.C., Moghimi, S.M., 2010. Cationic carriers of genetic material and cell death: a mitochondrial tale. Biochim. Biophys. Acta (BBA)-Bioenerg. 1797 (6-7), 1203–1209.
- Jevprasesphant, R., Penny, J., Jalal, R., Attwood, D., McKeown, N., D'emanuele, A., 2003. The influence of surface modification on the cytotoxicity of PAMAM dendrimers. Int. J. Pharm. 252, 263–266.
- Kim, T.-H., Choi, H., Yu, G.S., Lee, J., Choi, J.S., 2013. Novel hyperbranched polyethyleneimine conjugate as an efficient non-viral gene delivery vector. Macromol. Res. 21 (10), 1097–1104.
- Kirby, T.W., Gassman, N.R., Smith, C.E., Zhao, M.-L., Horton, J.K., Wilson, S.H., London, R.E., 2017. DNA polymerase β contains a functional nuclear localization signal at its N-terminus. Nucleic Acids Res. 45, 1958–1970.
- Lächelt, U., Wagner, E., 2015. Nucleic acid therapeutics using polyplexes: a journey of 50 years (and beyond). Chem. Rev. 115 (19), 11043–11078.
- Lee, M.-J., Cho, S.-S., You, J.-R., Lee, Y., Kang, B.-D., Choi, J.S., Park, J.-W., Suh, Y.-L., Kim, J.-A., Kim, D.-K., Park, J.-S., 2002. Intraperitoneal gene delivery mediated by a novel cationic liposome in a peritoneal disseminated ovarian cancer model. Gene Ther. 9 (13), 859–866.
- Lee, M.S., Kim, N.W., Lee, K., Kim, H., Jeong, J.H., 2013. Enhanced transfection by antioxidative polymeric gene carrier that reduces polyplex-mediated cellular oxidative stress. Pharm. Res. 30 (6), 1642–1651.
- Lee, J., Kwon, Y.-E., Kim, Y., Choi, J.S., 2021. Enhanced transfection efficiency of low generation PAMAM dendrimer conjugated with the nuclear localization signal peptide derived from herpesviridae. J. Biomater. Sci. Polym. Ed. 32 (1), 22–41.
- Lewis, L.M., Badkar, A.V., Cirelli, D., Combs, R., Lerch, T.F., 2023. The race to develop the pfizer-BioNTech COVID-19 vaccine: From the pharmaceutical scientists' perspective. J. Pharm. Sci. 112 (3), 640–647.
- Li, X., Hao, S., Han, A., Yang, Y., Fang, G., Liu, J., Wang, S., 2019. Intracellular Fenton reaction based on mitochondria-targeted copper (ii)-peptide complex for induced apoptosis. J. Mater. Chem. B 7, 4008–4016.
- Ma, C.-C., Wang, Z.-L., Xu, T., He, Z.-Y., Wei, Y.-Q., 2020. The approved gene therapy drugs worldwide: from 1998 to 2019. Biotechnol. Adv. 40, 107502.
- Macdonald, J., Galley, H.F., Webster, N.R., 2003. Oxidative stress and gene expression in sepsis. Br. J. Anaesth. 90 (2), 221–232.
- Monnery, B.D., Wright, M., Cavill, R., Hoogenboom, R., Shaunak, S., Steinke, J.H.G., Thanou, M., 2017. Cytotoxicity of polycations: Relationship of molecular weight and the hydrolytic theory of the mechanism of toxicity. Int. J. Pharm. 521 (1-2), 249–258.
- Mullard, A., 2023. 2022 FDA approvals. Nat. Rev. Drug Discov. 22 (2), 83-88.

- Naha, P.C., Davoren, M., Lyng, F.M., Byrne, H.J., 2010. Reactive oxygen species (ROS) induced cytokine production and cytotoxicity of PAMAM dendrimers in J774A. 1 cells. Toxicol. Appl. Pharmacol. 246 (1-2), 91–99.
- Nakamura, T., Sato, Y., Watanabe, D., Ito, H., Shimonohara, N., Tsuji, T., Nakajima, N., Suzuki, Y., Matsuo, K., Nakagawa, H., Sata, T., Katano, H., 2010. Nuclear localization of Merkel cell polyomavirus large T antigen in Merkel cell carcinoma. Virology 398 (2), 273–279.
- Nam, H.Y., Nam, K., Hahn, H.J., Kim, B.H., Lim, H.J., Kim, H.J., Choi, J.S., Park, J.-S., 2009. Biodegradable PAMAM ester for enhanced transfection efficiency with low cytotoxicity. Biomaterials 30 (4), 665–673.
- Park, E., Cho, H.-B., Takimoto, K., 2015. Effective gene delivery into adipose-derived stem cells: transfection of cells in suspension with the use of a nuclear localization signal peptide-conjugated polyethylenimine. Cytotherapy 17 (5), 536–542.
- Pollard, H., Remy, J.-S., Loussouarn, G., Demolombe, S., Behr, J.-P., Escande, D., 1998. Polyethylenimine but not cationic lipids promotes transgene delivery to the nucleus in mammalian cells. J. Biol. Chem. 273 (13), 7507–7511.
- Ren, T., Li, L., Cai, X., Dong, H., Liu, S., Li, Y., 2012. Engineered polyethylenimine/ graphene oxide nanocomposite for nuclear localized gene delivery. Polym. Chem. 3, 2561–2569.
- Shi, J., Chou, B., Choi, J.L., Ta, A.L., Pun, S.H., 2013b. Investigation of polyethylenimine/DNA polyplex transfection to cultured cells using radiolabeling and subcellular fractionation methods. Mol. Pharm. 10 (6), 2145–2156.
- Shi, B., Zhang, H.u., Shen, Z., Bi, J., Dai, S., 2013a. Developing a chitosan supported imidazole Schiff-base for high-efficiency gene delivery. Polym. Chem. 4 (3), 840–850
- Symonds, P., Murray, J.C., Hunter, A.C., Debska, G., Szewczyk, A., Moghimi, S.M., 2005. Low and high molecular weight poly (I-lysine) s/poly (I-lysine)—DNA complexes initiate mitochondrial-mediated apoptosis differently. FEBS Lett. 579, 6191–6198.
- Thuy, L.T., Mallick, S., Choi, J.S., 2015. Polyamidoamine (PAMAM) dendrimers modified with short oligopeptides for early endosomal escape and enhanced gene delivery. Int. J. Pharm. 492 (1-2), 233–243.
- Vera-Aviles, M., Vantana, E., Kardinasari, E., Koh, N.L., Latunde-Dada, G.O., 2018.
 Protective role of histidine supplementation against oxidative stress damage in the management of anemia of chronic kidney disease. Pharmaceuticals 11, 111.
- Wade, A.M., Tucker, H.N., 1998. Antioxidant characteristics of L-histidine. J. Nutr. Biochem. 9, 308–315.
- Wake, H., Takahashi, Y., Yoshii, Y., Gao, S., Mori, S., Wang, D., Teshigawara, K., Nishibori, M., 2020. Histidine-rich glycoprotein possesses antioxidant activity through self-oxidation and inhibition of hydroxyl radical production via chelating divalent metal ions in Fenton's reaction. Free Radic. Res. 54 (8-9), 649–661.
- Wang, Y.i., Bruggeman, K.F., Franks, S., Gautam, V., Hodgetts, S.I., Harvey, A.R., Williams, R.J., Nisbet, D.R., 2021. Is viral vector gene delivery more effective using biomaterials? Adv. Healthc. Mater. 10 (1), 2001238.
- Watts, J.K., Corey, D.R., 2012. Gene silencing by siRNAs and antisense oligonucleotides in the laboratory and the clinic. J. Pathol. 226, 365.
- Wing, C.E., Fung, H.Y.J., Chook, Y.M., 2022. Karyopherin-mediated nucleocytoplasmic transport. Nat. Rev. Mol. Cell Biol. 23 (5), 307–328.
- Xia, T., Kovochich, M., Liong, M., Zink, J.I., Nel, A.E., 2008. Cationic polystyrene nanosphere toxicity depends on cell-specific endocytic and mitochondrial injury pathways. ACS Nano 2 (1), 85–96.
- Yi, W.-J., Yang, J., Li, C., Wang, H.-Y., Liu, C.-W., Tao, L.i., Cheng, S.-X., Zhuo, R.-X., Zhang, X.-Z., 2012. Enhanced nuclear import and transfection efficiency of TAT peptide-based gene delivery systems modified by additional nuclear localization signals. Bioconjug. Chem. 23 (1), 125–134.
- Zhang, H., Liang, Z., Li, W., Li, F., Chen, Q., 2013. Nuclear location signal peptide–modified poly (ethyleneimine)/DNA complexes: An efficient gene delivery vector in vitro and in vivo. J. Bioact. Compat. Polym. 28 (3), 218–232.
- Zhang, H., Chen, Z., Du, M., Li, Y., Chen, Y., 2018. Enhanced gene transfection efficiency by low-dose 25 kDa polyethylenimine by the assistance of 1.8 kDa polyethylenimine. Drug Deliv. 25, 1740–1745.
- Zugates, G.T., Anderson, D.G., Little, S.R., Lawhorn, I.E.B., Langer, R., 2006. Synthesis of poly (β -amino ester) s with thiol-reactive side chains for DNA delivery. J. Am. Chem. Soc. 128 (39), 12726–12734.